Signal Separation and Target Localization for FDA Radar

CHUANZHI WANG[ID][1], **XIAOHUA ZHU**[1], **(Member, IEEE), AND XUEHUA LI**[2]

[1]School of Electronics and Optical Engineering, Nanjing University of Science and Technology, Nanjing 210094, China
[2]College of Electronics Engineering, Chengdu University of Information Technology, Chengdu 610225, China

Corresponding author: Chuanzhi Wang (wczmail@foxmail.com)

ABSTRACT Frequency diverse array (FDA) radar have attracted great interests due to the range-angle-dependent transmit beampattern which is different from phased array radar providing only angle-dependent transmit beampattern. In this paper, we firstly proposed a receiver processing strategy based on signal separation method which eliminates the need for employing a bank of bandpass filters at the receiver of FDA radar. In the proposed separation scheme, the received signal at each receiving element was separated into M channels, where M represents the transmitting element number. After time-invariant processing of the separated signal, the angle and range were estimated by two-stage multiple signal classification (MUSIC) algorithm. For velocity estimation, we proposed a novel unambiguous velocity estimation algorithm. This novel algorithm was implemented to calculate the phase of each element and then the differential phase within the adjacent elements is calculated. The velocity of the target was estimated by the differential phase. This mechanism for extending the Nyquist velocity range is that the differential phase of the two adjacent channels has a much smaller variance than the individual channel phase estimated. All estimated parameter performance is verified by analyzing the Cramér-Rao lower bound (CRLB) and the root mean square errors (RMSE).

INDEX TERMS Frequency diverse array (FDA) radar, signal separation, parameters estimation, target localization, fraction Fourier transform (FRFT).

I. INTRODUCTION

Phased array radar lies at the heart of many aspects of multi-target detection and interference suppression because it provides directional gain by steering its beam electronically. However, the drawback of the phased array is the range-independent transmit beampattern. The range-dependent beampattern plays a crucial role in mitigating the range interference and distinguishing the different range target in the desired direction. Fortunately, frequency diversity array (FDA) radar has received much attention in recent years due to its range-angle-dependent transmit beampattern properties since it was firstly proposed by Antonik *et al.* [1]. Differing from the traditional phased-array radar providing only angle-dependent transmit beampattern, the FDA radar applies a small frequency increment between

The associate editor coordinating the review of this manuscript and approving it for publication was Hasan S. Mir.

the transmit array elements which enable the array beam to scan without the need for expensive phase shifters. The FDA radar beampattern properties have many potential applications in radar anti-jamming, joint multi-parameter estimation, low probability if identification, cognitive radar, and electronic counter-countermeasures [2]–[4]. In 2012, Jones and Rigling [5] proposed three FDA receiver architectures, namely, band-limited coherent receiver, full-band pseudo-coherent receiver, and full-band coherent receiver, respectively. The full-band coherent architecture is widely used because it could process the information and energy of all the signal efficiently. However, this receiver architecture contains a filter bank at each receive element and each filter bank contains M narrowband filters which only see the signal with the same frequency. A novel receiver architecture [6] and a range-angle matched receiver [7] were proposed based on the full-band coherent receiver. However, these architectures are assumed that the frequency non-overlapping

waveforms of each transmit element. Cui *et al.* [8] utilized the frequency analysis method by taking discrete frequency transform (DFT), but this method is not suitable for wideband signals with overlapping spectrum such as linear frequency modulated (LFM) signal which is widely used in radar and communications.

More recently, there has been a growing number of researched focusing on FDA radar, especially in range-angle beampattern decoupling and beamforming and joint range-angle estimation of the target. For decoupling range-angle transmit pattern, some nonuniform frequency increment methods were investigated. Reference [9] proposed a rang-angle beam decoupled method with logarithmically increasing frequency offset. In [10], a random logarithmically increasing frequency offset was proposed to achieve a nonperiodic beampattern. In [11], a combining index modulation architecture with FDA was explored to decouple the range-angle beampattern with only one single peak. Reference [12] proposed an adaptively nonlinear optimal frequency increment selection method which can form a single peak beam at the target location. For beamforming of FDA radar, previous investigations have focused on the dot-shaped beamforming [13], [14]. Reference [15] build a closed-form and range-angle decoupled mathematical and designed a mathematically optimal method for FDA focusing beamforming. However, this dot-shaped beampattern is not suitable for range deceptive jamming suppression. To overcome this drawback, Liao *et al.* [16] proposed a weight designing technology to control the null distribution among range cells in the main beam.

When a lot of research on FDA rang-angle beampattern, there is also some research on joint range-angle estimation of FDA radar. Wang and Shao [17] proposed a simple and practical joint angle and range estimation method of transmitting double-pulse. The first pulse with zero frequency increment is used to estimate the direction of arrival and the second pulse with uniform frequency increment to estimate the range. However, this method didn't consider the full-band coherent receiver with full utilized spatial information. Subsequently, some research of joint range-angle estimation method with estimating signal parameters via rotational invariance techniques (ESPRIT) or multiple signal classification (MUSIC) algorithm have been explored [18], [19]. Tang *et al.* [20] proposed a girdles compressed sensing algorithm to joint estimate range-angle. Reference [21] estimated the range by applying standard spectral analysis and posed the angle estimation as a variant of the block sparse signal recovery problem. Xu *et al.* [22] transformed the joint range and angle estimation issues into a spectrum estimation problems and the minimum variance distortionless response (MVDR) algorithm used to jointly estimate the target range and angle. Wang *et al.* [23] designed a unfolded coprime array framework for FDA-MIMO radar, and constructed the joint angle and range estimation problem as a 2D-MUSIC spatial spectrum problem. Mu and Song [24] proposed a novel time-reversal approach for range-angle

estimation. However, these parameter estimation methods assume that the FDA receiver is a full-band coherent architecture for the monochromatic signal model and the receiving beampattern is time-invariant. Xu *et al,* [25], Xu and Xu [26] proposed an effective approach to resolve the time-varying issue of pulsed-FDA radar at the receiver and synthesize range-angle-dependent beampattern. References [27] and [28] were studied a time-modulated optimal frequency increment offset to obtain a time-independent transmit beampattern. Although a lot of research on angle and range estimation of FDA radar, there is little published information on the unambiguous velocity estimation of FDA radar. Recently, there has been some interest in robust radial estimation for FDA synthetic aperture radar (SAR). In 2019, Guo *et al.* [29] concentrated on a robust method on the condition of image coregistration and channel phase errors for FDA-SAR radar and He *et al.* [30] demonstrated a robust radial velocity estimation algorithm based on joint pixel normalized sample covariance matrix and shift vector. Unfortunately, these methods illustrated above are applied only to SAR radar and have higher computational complexity. Venkatesh *et al.* [31] presented a frequency diversity pulse pairs (FDPP) algorithm which is transmitted two short pulses with different carrier frequencies in sequence and exchanged the order of the pulse pairs in the next pulse repetition interval. Although the FDPP algorithm improves performance for maximum unambiguous velocity (MUV), it also results in the problem of non-uniform sampling and unable in FDA radar.

For the problems illustrated above, in this paper, we firstly proposed a signal separation-based method to obtain coherent receive signals. Unlike full-band coherent receiver architecture, the received signal after mixing of each receiving element was separated into M channel signals where M represents transmit element number. In order to obtain the time-invariant transmit-receive beampattern, the time-varying term in each separated signal can be eliminated with a designated mixer. Therefore, we no longer need to use sets of bandpass filters. The separated signals corresponding to the reference transmitting frequency were used to estimate the angle information by the MUSIC algorithm. The estimated angle was taken into the beampattern for range calculation. In addition, we derived a novel unambiguous velocity estimation formula which is not limited to the radar wavelength.

The remainder of this paper is organized as follows. Section ii introduces the signal model of FDA radar and the fraction Fourier transform. Approaches to separate and reconstruct of received signal and estimation of angle, range, and velocity are explored in Section iii. Section iv gave the numerical simulation and experimental results. Finally, conclusions are drawn in Section v.

II. FDA RADAR SIGNAL MODEL AND FRFT
A. FDA SIGNAL MODEL
Different from the traditional phased-array radar, the frequency diversity array radar adds a frequency increment Δf
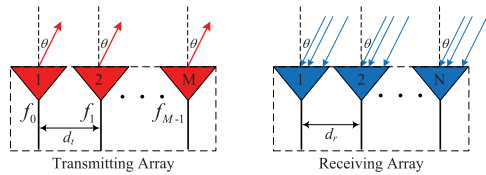
FIGURE 1. Geometry of M transmitting elements and N receiving elements frequency diversity array system.

to the transmitted signal that is much smaller than the radar operating carrier frequency on the adjacent element. The radiation frequency of the first element is f_0 which is the reference carrier frequency. The geometry of a frequency diversity array radar system with M transmitting elements and N receiving elements is shown in Fig.1. Assuming that the uniform transmitting and receiving element spacing is d. The radiated frequency of the m-th element is as follows:

$$f_m = f_0 + m\Delta f, \quad m = 0, \cdots, M-1 \quad (1)$$

where M is the number of transmitting element. The frequency increment Δf is negligible compared with the reference carrier frequency f_0. It should be emphasized that each element transmits a coherent signal. Thus, the received signal of each element consists of all the echoes transmitted from each element. The transmitted signal of the m-th element can be expressed as

$$s_m(t) = a_m \exp(j2\pi f_m t) e(t) \quad (2)$$

where a_m is a complex weighting factor that represents the unit-energy waveform of the n-th transmission and propagation effects that may be neglected (i.e., $a_m = 1$) for our purposes and $e(t) = exp(j\pi\mu t^2)$ is the linear frequency modulated (LFM) signal and μ is the chirp rate. Considering a far-field point located at (θ, r), where θ and r represent the direction of arrival and the slant range of the target, respectively. The received echo by the n-th receiving element through target backscattering can be expressed as Eq.(3):

$$x_n(t, r, \theta) = \sum_{m=0}^{M-1} q \exp\{j2\pi f_m(t - \tau_{nm})\} e(t - \tau_{nm}) + n_n(tf)$$
$$(3)$$

where $n_n(t)$ represents the additive white Gaussian noise of the n-th receiving element and q denotes the complex amplitudes of the target signal. Where τ_{nm} represents the time delay from the m-th transmitting element to the target and returning to the n-th receiving element, it can be written as:

$$\tau_{nm} = \frac{2r - md\sin\theta - nd\sin\theta}{c} \quad (4)$$

For simplicity, suppose $e(t - \tau_{nm}) \approx e(t - \tau)$, where τ denotes the signal propagation time-delay of the reference element. After down-conversion with the frequency f_0, the received signal of the n-th receiving element can be expressed as:

$$\tilde{x}_n(t, r, \theta) = [a_{mr}(\theta) a_t(\theta, r)] c(t) + n_n(t) \quad (5)$$

where

$$c(t) = q\exp\left(j2\pi f_0 \frac{2r}{c}\right) \sum_{m=0}^{M-1} \{e(t - \tau) \exp(j2\pi m\Delta ft)\}$$

$$a_t(\theta, r) = \left[1, \cdots, \exp\left(j2\pi\left(\frac{f_m md\sin\theta - 2rm\Delta f}{c}\right)\right)\right]^T$$

$$a_{mr}(\theta) = \exp\left(j2\pi f_0\frac{nd\sin\theta}{c}\right) ones(1, M)$$

Note that $f_0 \gg \Delta f$, $a_{mr}(\theta)$ is an approximate expression. The received signals of all receiving elements expressed as:

$$X_{observe}(t, r, \theta) = [\tilde{x}_1, \cdots, \tilde{x}_n, \cdots, \tilde{x}_N]^T \quad (6)$$

where $X_{observe} \in \mathbb{C}^{N\times L}$, N denotes the receiving element number and L denotes the snapshot number.

B. SIGNAL PROPERTY

For FDA radar, the received signal of each receiving element are the sum of all echo signals which was transmitted from each transmitting element. After down-conversion of the receiving signal with the local frequency f_0, the signal can be regarded as the superposition of multiple LFM signals. For frequency non-overlapping LFM whose frequency increment Δf is larger than the bandwidth B of the LFM signal, these signals can be separated by match filter of full-band coherent receiver [5] or discrete frequency transform (DFT) analysis [8]. However, for frequency overlapping LFM signal whose frequency increment Δf is less than or equal to the bandwidth B of the LFM signal, the match filter of the full-band coherent receiver and DFT technology is incapable. The fraction Fourier transform (FRFT) can be interpreted as a rotation of signals in the time-frequency plane and serves as an orthonormal signal representation for chirp signals [31]. In this paper, the received echo signal of each receiving element is processed by down-conversion with the local frequency f_0, analog-to-digital conversion, and signal separation with FRFT. The general processing sketch is shown in Fig.2.

C. FRFT SIGNAL SEPARATION

The fraction Fourier transform (FRFT) of a signal $h(t)$ is defined as:

$$H_p(u) = \int_{-\infty}^{+\infty} h(t)\kappa_p(u, t)dt \quad (7)$$

where $\kappa_p(u, t)$ is the transform kernel, and if $\alpha \neq k\pi$, $\kappa_p(u, t) = A_\alpha exp\{j\pi[(u^2 + t^2)\cot\alpha - 2utcsc\alpha]\}$; if $\alpha = 2k\pi$, $\kappa_p(u, t) = \delta(t - u)$; if $\alpha = (2k + 1)\pi$, $\kappa_p(u, t) = \delta(t - u)$. Where $A_\alpha = \sqrt{(1 - j\cot\alpha)/2}$, $\alpha = p\pi/2$ indicates the rotation angle of the transformed signal for FRFT, p is the transform order of the FRFT and a real number, and the FRFT operator is designated by H_p. For an LFM signal $h(t) = A\exp\left[j\pi\left(2f_0t + kt^2\right)\right]$, When $\alpha \neq k\pi$, the FRFT of LFM signal can be expressed as:

$$H_p(u) = AA_\alpha \int_{-\infty}^{+\infty} \exp\{j\pi[2(f_0 - u\csc\alpha)t$$
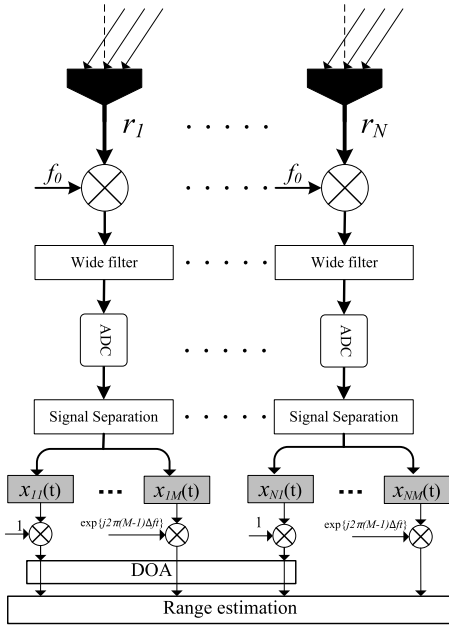$$+ (k + \cot\alpha)t^2 + u^2\cot\alpha]\}dt \quad (8)$$

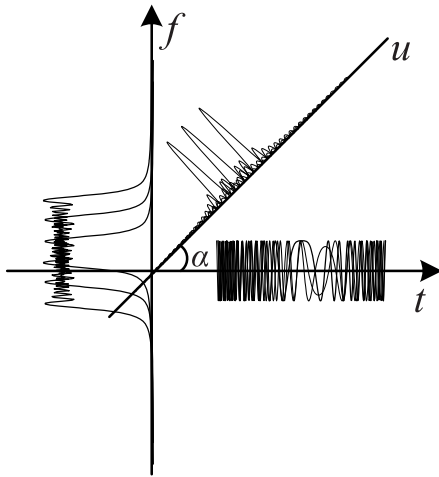**FIGURE 2.** Signal processing sketch at the receiver with signal separation.

FIGURE 3. The time-frequency of multi-component LFM signal and its projection to optimal fraction Fourier plane.

When $\alpha = arccot(-k)$, and $h(t)$ is an infinite signal, the formula degenerates to

$$H_p(u) = AA_\alpha \exp\left(j\pi u^2 \cot\alpha\right) \delta\left(f_0 - u \csc\alpha\right) \quad (9)$$

When $f_0 = \mu\csc\alpha$, the formula above is a Dirac function δ. For the received signal of each receiving element after mixing in this paper, each LFM signal component has the same chirp rate and difference initial frequency. The FRFT of these signals will have the same optimal rotation angle and will accrue multiple peaks which represent different initial frequency. Fig.3 shows three LFM signals with the same chirp rate and different initial frequency in time-domain and frequency-domain and fraction-domain. This Figure reveals that the multicomponent LFM signal with different peak in optimal fraction plane making signal separation possible.

Assuming that the separated signal in optimal fraction plane is H_{np}, the reconstructed signal can be derived by inverse FRFT of H_{np} as:

$$h_n(t) = \int_{-\infty}^{+\infty} H_{np}(u)\kappa_{-p}(t, u)du \quad (10)$$

III. RANGE, ANGLE, AND VELOCITY ESTIMATION

The FDA radar results in a time-variant range-angle-dependent transmit/receive beampattern because of frequency increment. However, the time-varying characteristics of beampattern increase the difficulty of FDA radar in beam steering and parameter estimation in snapshot. In this paper, a phase compensation approach is proposed to solve the time-varying problem of receiving signals. With the FRFT separation algorithm, the signal received by each receiving element is independently separated. The separated n-th signal of the m-th receiver channel can be expressed as:

$$\tilde{x}_{nm}(t) = qe(t - \tau)\exp(j2\pi m\Delta ft)\, a_t(\theta, r)\, a_r(\theta, n) \quad (11)$$

where $a_t(\theta, r) = \exp(j2\pi(\frac{f_m md \sin\theta - 2rm\Delta f}{c}))$ and $a_r(\theta) = \exp(j2\pi f_0 \frac{nd \sin\theta}{c})$, $\tilde{x}_{nm}(t)$ is mixed with the m-th mixer whose local frequency is $m\Delta f$ in accordance. Therefore, $\tilde{x}_{nm}(t)$ is converted into $\hat{x}_{nm}(t)$ which can be expressed as:

$$\begin{aligned} \hat{x}_{nm} &= \tilde{x}_{nm}(t) \times \exp\{-j2\pi m\Delta ft\} \\ &= qe(t - \tau_{nm})\, a_t(\theta, r)\, a_r(\theta, n) \end{aligned} \quad (12)$$

From this, we can see that the time-varying term in the steering vector is removed in this procedure. After separation and time-invariant processing, the rearranged echo signals can be rewritten as:

$$X = \left[\hat{x}_{11}, \cdots, \hat{x}_{1M}, \hat{x}_{21}, \cdots, \hat{x}_{2M}, \cdots, \hat{x}_{NM}\right] \quad (13)$$

where M represents the transmitting element number and N represents the receiving element number, the matrix $X \in \mathbb{C}^{NM \times L}$, and L represents the snapshot number. The received signal can be denoted as the matrix:

$$X = qA(\theta, r)e(t - \tau) + N \quad (14)$$

where $A \in \mathbb{C}^{NM \times 1}$ is the steering vector matrix, and N is the noise matrix.

$$A(\theta, r) = [a_r(\theta) \otimes a_t(\theta, r)]^T \quad (15)$$

where $a_r(\theta) = \left[1, \cdots, \exp\left(j2\pi f_0 \frac{(N-1)d \sin\theta}{c}\right)\right]$ denotes the steering matrix, $\otimes$ denotes the Kronecker product operator.

A. ANGLE ESTIMATION

The target direction of arrival can be estimated by utilizing the received echo signals which are radiated from the same transmitting element. In this section, we selected the rearranged signals, which are radiated from the reference element, $\tilde{X} = \left[\hat{x}_{11}, \hat{x}_{21}, \cdots, \hat{x}_{N1}\right]$ can be rewritten as:

$$\tilde{X} = a^T_r(\theta)\, qe(t - \tau) + \tilde{N} \quad (16)$$

where $\tilde{X} \in \mathbb{C}^{N \times L}$, and then the covariance matrix of $\tilde{X}$ can be expressed as:

$$R_{\tilde{X}} = E\left\{\tilde{X}\tilde{X}^H\right\} = AR_S A^H + \sigma^2 I_N \quad (17)$$

where $R_{\tilde{X}} \in {}^{N \times N}$ and R_s is the signal covariance matrix. For independent target signal and noise, the covariance matrix $R_{\tilde{X}}$ can be decomposed as

$$R_{\tilde{X}} = U_S \Lambda_S U_S^H + U_{\tilde{n}} \Lambda_{\tilde{n}} U_{\tilde{n}}^H \quad (18)$$

where the U_S and U_n denote the eigenvectors that span the signal subspace and the noise subspace column vectors of $R_{\tilde{X}}$, and the corresponding eigenvalues are Λ_S and Λ_n, respectively. When the signal covariance matrix $R_{\tilde{X}}$ is nonsingular and the column vectors of A are linearly independent, the steering vectors will span the same subspace as the signal subspace. In this case, the target angle can be estimated from the following expression:

$$\hat{\theta} = \arg\left\{\min_{\theta}\left[a_r^H(\theta) U_{\tilde{n}} U_{\tilde{n}}^H a_r(\theta)\right]\right\} \quad (19)$$

B. RANGLE ESTIMATION

When the angle of the target is estimated, the covariance matrix of the separated signal matrix X can be written as:

$$R_X = E\left\{XX^H\right\} = AR_S A^H + \sigma^2 I_{NM} \quad (20)$$

where $R_X \in \mathbb{C}^{NM \times NM}$ and R_S is the signal covariance matrix. For independent target signal and noise, the covariance matrix R_X can be decomposed as

$$R_X = U_S \Lambda_S U_S^H + U_n \Lambda_n U_n^H \quad (21)$$

We put the angle information θ estimated from Eq. (19) into the $A(\theta, r)$, the range can be estimated as follow expression:

$$\hat{r} = \arg\left\{\min_{r}\left[a^H\left(\hat{\theta}, r\right) U_n U_n^H a\left(\hat{\theta}, r\right)\right]\right\} \quad (22)$$

where $a(\hat{\theta}, r) = a_r(\hat{\theta}) \otimes a_t(\hat{\theta}, r)$. However, the estimated range by MUSIC algorithm will accrue range ambiguous because of the range-angle coupled beampattern. In this time, we can joint the pulse compression method to eliminate the folding range.

C. UNAMBIGUOUS VELOCITY ESTIATION

Assuming that a far-field target of the range r, the direction of arrival θ, and the velocity v, the demodulated baseband separated signal, which is transmitted from the m-th element, of the reference receiving element can be written as:

$$x_m(t) = \exp\{-j2\pi[f_d t + f_m(\frac{2r - 2md\sin\theta}{c})]\} \quad (23)$$

The demodulated signal consists of the Doppler frequency and element increment frequency and the target location delay. The Doppler frequency can be expressed as:

$$f_d = \frac{2f_m v}{c} = \frac{2v}{\lambda_m} \quad (24)$$

If the pulse width lasts long enough, $f_d < 1/T_p$, where T_p represents the pulse duration, the Doppler frequency can be exacted within a pulse width time. On the contrary, multiple pulse echoes within a coherent processing interval need to be processed to extract the Doppler frequency. Therefore, the general radar Doppler frequency information is extracted in the slow time domain. The demodulated target Doppler signals of the m-th transmitting element in the slow-time domain can be expressed as:

$$y_m(l) = \mu_m \exp\left(j2\pi \frac{2vf_m lPRT}{c}\right) + n(t) \quad (25)$$

where μ_m is the target signal amplitude, PRT is the pulse repetition time (PRT) which is the reciprocal of the pulse repetition frequency (PRF) and l is the pulse count of PRT, and $n(t)$ denotes the additive white noise. The correlation function of $y_m(l)$ and $y_m(l+1)$ can be expressed as:

$$R_m(l) = \overline{y_m(l) \times y_m{}^*(l+1)} \quad (26)$$

And then, the phase of the target modulated signal can be expressed as:

$$\varphi_{f_m} = \arg[R_m] = \frac{4\pi vPRTf_m}{c} \quad (27)$$

Similarly, the target echo signal phase of the (m+1)-th transmitting element also can be derived. Assuming that the differential phase of adjacent receive element is

$$\Delta\varphi = \varphi_{f_{m+1}} - \varphi_{f_m} = \frac{4\pi vPRT\Delta f}{c} \quad (28)$$

However, this method ignores the possibility that when the radial velocity value lies between these two MUV of the adjacent elements. Assume that v_{max1} and v_{max2} represent the maximum unambiguous velocity of radiated frequency f_1 and f_2, repetitively. If $v_{max2} < v < v_{max1}$, the differential phase $\Delta\varphi$ of the adjacent transmitting element channel will be out of the range of $[-\pi, \pi]$. In this case, the differential phase $\Delta\varphi$ needs to be modified as Eq.(29).

$$\Delta\varphi_m = \begin{cases} \Delta\varphi - 2\pi; & \Delta\varphi > \pi \\ \Delta\varphi + 2\pi; & \Delta\varphi < -\pi \end{cases} \quad (29)$$

Subsequently, the velocity of the target can be estimated as:

$$v = \frac{c\Delta\varphi}{\Delta f 4\pi PRT} \quad (30)$$

When the $\Delta\varphi = \pm\pi$, the maximum unambiguous velocity is:

$$v_{max} = \pm\frac{c}{4\Delta fPRT} \quad (31)$$

The maximum is inversely proportional to the product of increment frequency Δf and pulse repetition time PRT. For this parameter estimation algorithm, the product of the unambiguous range and velocity is not limited by the radar wavelength. The implement of this algorithm is based on the pulse-pairs algorithm for its superior performance in real-time computation. The summarized implement as Fig.4.
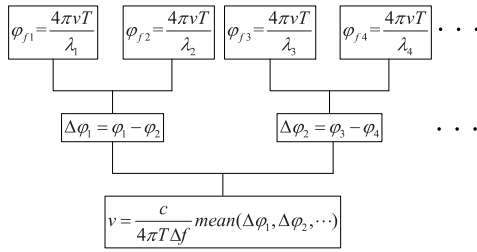
FIGURE 4. The proposed velocity estimation algorithm implementation processing sketch.

D. CARMÉR-RAO BOUND

To derive the Carmér-Rao Bound simply, the data models expressed in Eq.(14) and Eq.(16) can be rewritten as

$$y_{\theta,r} = \sqrt{SNR} \cdot b(\theta, r) + n \tag{32}$$

where the $(N + MN) * 1$ vector $b(\theta, r) = [a_r(\theta), A(\theta, r)]^T$ is the equivalent transmitting-receiving vector, and n is the Gaussian noise vector with zero mean and unit variance I. The corresponding Fisher information matrix (FIM) with parameters vector to be estimated $[\theta, r]$ is expressed as:

$$F_{\theta,r} = 2Re\left[\left(\frac{\sqrt{SNR}\partial b(\theta, r)}{\partial(\theta, r)}\right)^H \Gamma^{-1} \left(\frac{\sqrt{SNR}\partial b(\theta, r)}{\partial(\theta, r)}\right)\right] \tag{33}$$

The $CRLB_{\theta,r}$ is the inverse of FIM:

$$CRLB_{\theta,r} = F_{\theta,r}^{-1} \tag{34}$$

For velocity estimation, the data model can be rewritten as:

$$y_v = \sqrt{SNR}[y_1, y_2, \cdots, y_m]^T + n \tag{35}$$

where n denotes the additive white noise vector and $y_m = exp(j2\pi f_d lPRT)$. the corresponding Fisher information matrix (FIM) is expressed as:

$$F_v = 2Re\left[\left(\frac{\partial y_v}{\partial(v)}\right)^H \Gamma^{-1} \left(\frac{\partial y_v}{\partial(v)}\right)\right] \tag{36}$$

The $CRLB_v$ is the inverse of FIM:

$$CRLB_v = F_v^{-1} \tag{37}$$

IV. SIMULATION AND ANALYSIS

In this section, simulation experiments are operated to evaluate the effectiveness of the proposed strategy and algorithm in this paper. We simulate a uniform linear array with 8 transmitting elements and 8 receiving elements which elements spacings are the half wavelength at frequency $f_0 = 10GHz$. The band-width and time-width of the LFM signal are designed as $B = 2MHz$ and $T = 200us$, respectively. We assume that the frequency increment $\Delta f = 100KHz$, and sampling frequency $f_s = 4B$. For the direction of arrival and range estimation, we set the snapshots $L = 150$. For velocity estimation, we set the pulse number of coherent integration 64 and the pulse repetition frequency $PRF = 1000Hz$.
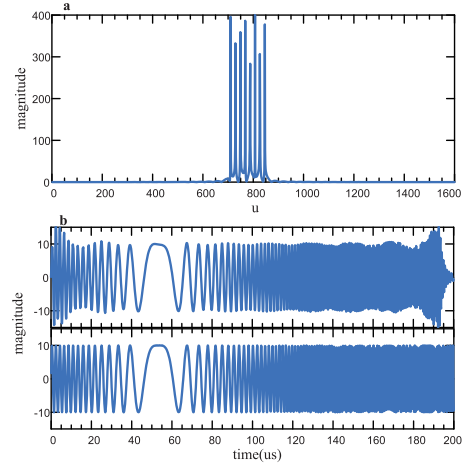

FIGURE 5. a). The optimal fraction plane with received signal of m-th element and b). The reconstructed signal.

A. SIGNAL SEPARATION OF FRFT

A fast discrete FRFT algorithm was proposed in 1996 by Ozaktas *et al.* [33], and it has become one of the usual discrete FRFT algorithms because of its low computational load and high accuracy. For the received echo LFM signal, the time-plane representation is constrained to the interval $[-T/2, T/2]$, and the frequency-plane representation is constrained to the interval $[-f_s/2, f_s/2]$. These two planes have different dimensions; therefore, the original signal must be normalized before the discrete FRFT computation. In order to transform the time-plane and frequency-plane to the plane with the same dimension, Reference [34] proposed two practical dimensional normalization methods: the discrete scaling and the data zero-padding/interception method. In this paper, the discrete scaling method was utilized and the dimensional normalization parameter $S = (T/f_s)^{1/2}$. After dimensional normalization, the chirp rate μ and optimal fractional rotation α of the received LFM signal have been changed. From [34], we know the new optimal fractional rotation angle $\hat{\alpha} = arccot(-\mu S^2)$, where $\mu = B/T$. According to the parameter given above, the new optimal fractional rotation angle is used to do fractional Fourier transform to obtain the fractional spectrum. Fig.5(a) shows the fractional spectrum in the optimal fractional domain and reveals that there are 8 peaks that represent the different initial frequency of echo LFM signal. Every peak is extracted for inverse fractional Fourier transform with parameter $-\hat{\alpha}$ to reconstruct the LFM signal with different frequency increment. The reconstructed signal which is received by the 1-th receiving element and transmitted by the 3-th transmitting element as Fig.5(b). As indicated in Fig.5(b), the reconstructed result is qualitatively similar to the ideal echo signal. All reconstructed signals after time-varying term eliminating of each receiving element are equivalent to the output of full-band match filters.

B. ANGLE AND RANGE ESTIMATION

The echo signals received by each receiving element are converted into *MN* channel signals after down-conversion,
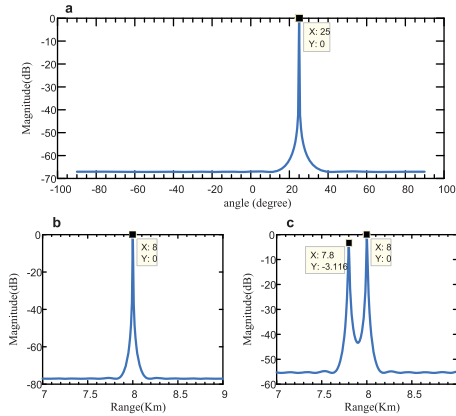
FIGURE 6. The pseudo spectrum of angle estimation and range estimation with MUSIC algorithm. a). The angle estimation. b). The range estimation of one target. c). The range estimation of two target with the same DOA.

FRFT separation and time-varying term eliminating. Since the coupling of beampattern, although the FDA radar provides a range-angle-dependent beampattern, the range and angle information cannot be estimated directly. According to Wang and Shao [17], the angle information can be estimated with zero frequency increment of FDA radar which operates as a phased array radar and the range information can be estimated with a non-zero frequency increment of FDA radar. In our study, the separated signals which are launched from the same transmitting element are combined for angle estimation and all the separated signals are interpreted to estimate range information. The experiment was considered in two scenes. **Scene one**: one target is located at $(25°, 8.0Km)$. The estimated angle pseudo spectrum is represented in Fig.6(a) and the estimated range is represented in Fig.6(b). The target can be easily located in the angle-range dimension as $(25°, 8.0Km)$. Note that the range ambiguous can be solved joint the conventional pulse compression algorithm and this range estimation approach. **Scene two**: two targets with the same angle but different range are located at $(25°, 7.8Km)$ and $(25°, 8.0Km)$, respectively. Fig.6(c) shows the target response of the estimated range profile. The two targets can be easily located at $(25°, 7.8Km)$ and $(25°, 8.0Km)$ which is can't be separated with a phased array radar.

C. VELOCTY ESTIMATION

Similar to the angle estimation mentioned above, the separated signals with the same transmitting element emission are combined for angle estimation. The difference of the angle estimation is that the velocity estimation is processed in the slow-time domain. The pulse repetition frequency (PRF) is $1000Hz$ which the corresponding maximum unambiguous velocity by traditional algorithm is $±7.5m/s$. In order to verify the effectiveness of unambiguous velocity estimation with the method proposed in this paper, we assume two targets with the same location as scene two in range estimation and velocity of $-550m/s$ and $1000m/s$, respectively. Fig.7 shows the velocity estimation results as the red circle and the range of velocity estimated without ambiguous as the blue curve.
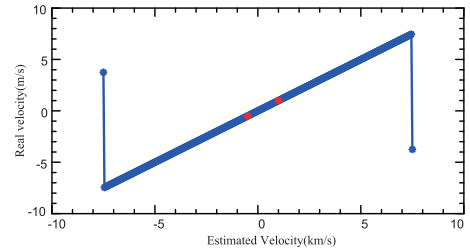

FIGURE 7. The velocity estimation results with two targets and the range of velocity estimation with the parameters above.
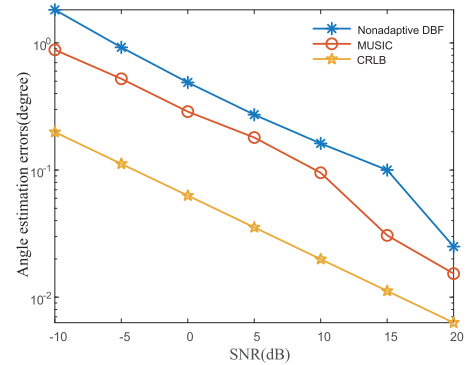

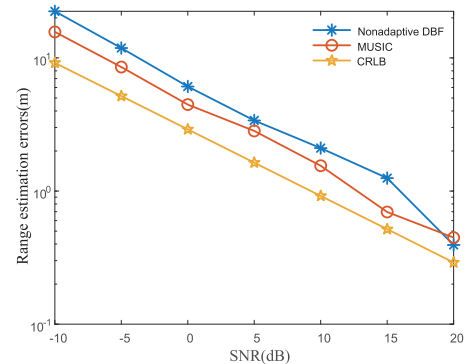**FIGURE 8.** The DOA estimation performance versus SNR.

FIGURE 9. The range estimation performance versus SNR.

The velocity of two targets can be easily visible as $-550m/s$ and $1000m/s$.

D. ROOT MEAN SQUARE ERRORS

To assess the performance of the angle, range, and velocity estimations, the root mean square errors (RMSE) was employed. The definition of $RMSE_\theta$, $RMSE_r$, and $RMSE_v$ is expressed as follows:

$$RMSE_\theta = \frac{1}{D}\sum_{i=1}^{D}\sqrt{\frac{1}{L}\sum_{l=1}^{L}\left(\hat{\theta}_i - \theta_i\right)} \quad (38)$$

$$RMSE_r = \frac{1}{D}\sum_{i=1}^{D}\sqrt{\frac{1}{L}\sum_{l=1}^{L}\left(\hat{r}_i - r_i\right)} \quad (39)$$
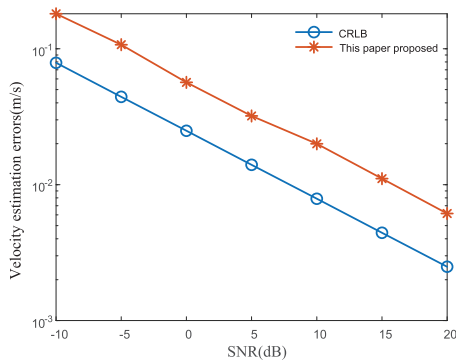
FIGURE 10. The velocity estimation performance versus SNR.

$$RMSE_v = \frac{1}{D} \sum_{i=1}^{D} \sqrt{\frac{1}{L} \sum_{l=1}^{L} (\hat{v}_i - v_i)} \qquad (40)$$

where θ, r, v is the estimated angle, range, and velocity, respectively. The target number $D = 2$ and the number of Monte-Carlo independent trials $L = 200$. Fig.8 and Fig.9 and Fig.10 correspond to the RMSEs of angle and range and velocity estimation with different SNR for different estimation algorithms. The CRLB and RMSEs of the angle and range estimation comparison with the approach proposed in this paper and the method by Reference [17] are displayed in Fig.8 and 9, respectively. The comparison of RMSEs between the proposed algorithm and CRLB with difference SNR shown in Fig.10.

V. CONCLUSION

FDA radar has been studied extensively in recent years, however, there is a surprising paucity of empirical research focusing on received signal processing and parameters estimation. In this paper, we have proposed a common framework for FDA radar received signal processing which can be interpreted as signal separation instead of full-band coherent matched filter and the target localizing in angle and range dimension and then detecting the target velocity. Since the LFM signals which are frequency overlapping were designed for FDA transmitting element, the FRFT technology is used to separate the received multi-component LFM signal of each receiving element. After signal separating, each single component LFM signal can be effectively reconstructed. The angle and range parameters are estimated by the classical MUSIC algorithm and the velocity is estimated by the proposed algorithm in this paper. The parameters estimation performance is presented by comparing the RMSE, CRLB, and the nonadaptive beamformer. Certainly, we think the blind source separation technology that exists in the literature can provide new application potentials in received signal separation and the optimal estimator also can present an improved performance in parameters estimation. The adaptive beamforming technology also can be investigated in FDA radar with signal separation. Therefore, future work should include the blind source separation technology and adaptive beamforming application and evaluation in FDA radar.

REFERENCES

[1] P. Antonik, M. C. Wicks, H. D. Griffiths, and C. J. Baker, "Frequency diverse array radars," in *Proc. IEEE Radar Conf.*, Verona, NY, USA, Apr. 2006, pp. 215–217.

[2] A. Basit, W. Khan, S. Khan, and I. M. Qureshi, "Development of frequency diverse array radar technology: A review," *IET Radar, Sonar Navigat.*, vol. 12, no. 2, pp. 165–175, Feb. 2018.

[3] A. Abdalla, H. Abdalla, M. Ramadan, S. Mohamed, and T. Bin, "Overview of frequency diverse array in radar ECCM applications," in *Proc. Int. Conf. Commun., Control, Comput. Electron. Eng.*, Khartoum, Sudan, Jan. 2017, pp. 1–7.

[4] W.-Q. Wang, "Overview of frequency diverse array in radar and navigation applications," *IET Radar, Sonar Navigat.*, vol. 10, no. 6, pp. 1001–1012, Jul. 2016.

[5] A. M. Jones and B. D. Rigling, "Frequency diverse array radar receiver architectures," in *Proc. Int. Waveform Diversity Design Conf. (WDD)*, Kauai, HI, USA, Jan. 2012, pp. 211–217.

[6] S. Han, C. Fan, and X. Huang, "A novel receiver architecture for frequency diverse array radar," in *Proc. Prog. Electromagn. Res. Symp.*, Shanghai, China, Aug. 2016, pp. 2270–2274.

[7] J. Xu, L. Lan, G. Liao, and Y. Zhang, "Range-angle matched receiver for coherent FDA radars," in *Proc. IEEE Radar Conf. (RadarConf)*, Seattle, WA, USA, May 2017, pp. 0324–0328.

[8] C. Cui, J. Xiong, W.-Q. Wang, and W. Wu, "Localization performance analysis of FDA radar receiver with two-stage estimator," *IEEE Trans. Aerosp. Electron. Syst.*, vol. 54, no. 6, pp. 2873–2887, Dec. 2018.

[9] W. Khan, I. M. Qureshi, and S. Saeed, "Frequency diverse array radar with logarithmically increasing frequency offset," *IEEE Antennas Wireless Propag. Lett.*, vol. 14, pp. 499–502, 2015.

[10] G. Huang, Y. Ding, S. Ouyang, and V. Fusco, "Frequency diverse array with random logarithmically increasing frequency offset," *Microw. Opt. Technol. Lett.*, vol. 62, no. 7, pp. 2554–2561, Jul. 2020.

[11] G. Huang, S. Ouyang, Y. Ding, and V. Fusco, "Index modulation for frequency diverse array," *IEEE Antennas Wireless Propag. Lett.*, vol. 19, no. 1, pp. 49–53, Jan. 2020.

[12] H. Chen, R. Li, L. Dai, and Y. Shao, "A nonlinear FDA optimal frequency increment selection method," in *Proc. IEEE 3rd Int. Conf. Signal Image Process.*, Jul. 2018, pp. 452–456.

[13] Y. Xu, X. Shi, W. Li, J. Xu, and L. Huang, "Low-sidelobe range-angle beamforming with FDA using multiple parameter optimization," *IEEE Trans. Aerosp. Electron. Syst.*, vol. 55, no. 5, pp. 2214–2225, Oct. 2019.

[14] B. Wang, J. Xie, J. Zhang, and H. Zhang, "Dot-shaped beamforming analysis based on OSB log-FDA," *J. Syst. Eng. Electron.*, vol. 31, no. 2, pp. 312–320, Apr. 2020.

[15] Y. Ma, P. Wei, and H. Zhang, "General focusing beamformer for FDA: Mathematical model and resolution analysis," *IEEE Trans. Antennas Propag.*, vol. 67, no. 5, pp. 3089–3100, May 2019.

[16] Y. Liao, H. Tang, X. Chen, W.-Q. Wang, M. Xing, Z. Zheng, J. Wang, and Q. H. Liu, "Antenna beampattern with range null control using weighted frequency diverse array," *IEEE Access*, vol. 8, pp. 50107–50117, Mar. 2020.

[17] W.-Q. Wang and H. Shao, "Range-angle localization of targets by a double-pulse frequency diverse array radar," *IEEE J. Sel. Topics Signal Process.*, vol. 8, no. 1, pp. 106–114, Feb. 2014.

[18] Y. Yan, J. Cai, and W.-Q. Wang, "Two-stage ESPRIT for unambiguous angle and range estimation in FDA-MIMO radar," *Digit. Signal Process.*, vol. 92, pp. 151–165, Sep. 2019.

[19] Y. Song, G. Zheng, and G. Hu, "A combined ESPRIT-MUSIC method for FDA-MIMO radar with extended range ambiguity using staggered frequency increment," *Int. J. Antennas Propag.*, vol. 2019, pp. 1–7, Jul. 2019.

[20] W.-G. Tang, H. Jiang, and Q. Zhang, "Range-angle decoupling and estimation for FDA-MIMO radar via atomic norm minimization and accelerated proximal gradient," *IEEE Signal Process. Lett.*, vol. 27, pp. 366–370, Feb. 2020.

[21] K. Mahata and M. M. Hyder, "Parametric localisation in frequency diverse array," *IET Radar Sonar Navigat.*, vol. 14, no. 5, pp. 716–727, May 2020.

[22] J. Xu, G. Liao, S. Zhu, L. Huang, and H. C. So, "Joint range and angle estimation using MIMO radar with frequency diverse array," *IEEE Trans. Signal Process.*, vol. 63, no. 13, pp. 3396–3410, Jul. 2015.

[23] C. Wang, Z. Li, and X. Zhang, "FDA-MIMO for joint angle and range estimation: Unfolded coprime framework and parameter estimation algorithm," *IET Radar, Sonar Navigat.*, vol. 14, no. 6, pp. 917–926, Jun. 2020.

[24] T. Mu and Y. L. Song, "Target range-angle estimation based on time reversal FDA-MIMO radar," *Int. J. Microw. Wireless Technol.*, vol. 12, no. 4, pp. 267–275, May 2020.

[25] Y. Xu, X. Shi, J. Xu, and P. Li, "Range-angle-dependent beamforming of pulsed frequency diverse array," *IEEE Trans. Antennas Propag.*, vol. 63, no. 7, pp. 3262–3267, Jul. 2015.

[26] Y. Xu and J. Xu, "Corrections to 'range-angle-dependent beamforming of pulsed-frequency diverse array,'" *IEEE Trans. Antennas Propag.*, vol. 66, no. 11, pp. 6466–6468, Nov. 2018.

[27] W. Khan and I. M. Qureshi, "Frequency diverse array radar with time-dependent frequency offset," *IEEE Antennas Wireless Propag. Lett.*, vol. 13, pp. 758–761, 2014.

[28] A.-M. Yao, P. Rocca, W. Wu, A. Massa, and D.-G. Fang, "Synthesis of time-modulated frequency diverse arrays for short-range multi-focusing," *IEEE J. Sel. Topics Signal Process.*, vol. 11, no. 2, pp. 282–294, Mar. 2017.

[29] Y. Guo, G. Liao, Q. Zhang, J. Li, and T. Gu, "A robust radial velocity estimation method for FDA-SAR," *IEEE Geosci. Remote Sens. Lett.*, vol. 17, no. 4, pp. 646–650, Jul. 2019.

[30] X. He, G. Liao, J. Xu, and S. Zhu, "Robust radial velocity estimation based on joint-pixel normalized sample covariance matrix and shift vector for moving targets," *IEEE Geosci. Remote Sens. Lett.*, vol. 16, no. 2, pp. 221–225, Feb. 2019.

[31] V. Venkatesh, L. Li, M. McLinden, M. Coon, G. M. Heymsfield, S. Tanelli, and H. Hovhannisyan, "A frequency diversity algorithm for extending the radar Doppler velocity Nyquist interval," *IEEE Trans. Aerosp. Electron. Syst.*, vol. 56, no. 3, pp. 2462–2470, Jun. 2020.

[32] R. Tao, F. Zhang, and Y. Wang, "Fractional power spectrum," *IEEE Trans. Signal Process.*, vol. 56, no. 9, pp. 4199–4206, Sep. 2008.

[33] H. M. Ozaktas, O. Arikan, M. A. Kutay, and G. Bozdagt, "Digital computation of the fractional Fourier transform," *IEEE Trans. Signal Process.*, vol. 44, no. 9, pp. 2141–2150, Sep. 1996.

[34] X. Zhao, T. Ran, and D. Bing, "Practical normalization methods in the digital computation of the fractional Fourier transform," in *Proc. 7th Int. Conf. Signal Process.*, New York, NY, USA, Sep. 2004, pp. 105–108.

CHUANZHI WANG received the M.E. degree in electronics and communication engineering from the College of Electronics Engineering, Chengdu University of Information Technology, Chengdu, China, in 2018. He is currently pursuing the Ph.D. degree in information and communication engineering with the School of Electronics and Optical Engineering, Nanjing University of Science and Technology, Nanjing, China. His current research interests include digital signal processing, radar anti-jamming technology, and frequency diversity array radar systems.
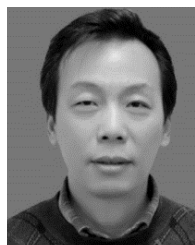
XIAOHUA ZHU (Member, IEEE) received the Ph.D. degree in communication and information systems from the Nanjing University of Science and Technology, Nanjing, China, in 2002.

He is currently a Professor with the School of Electronics and Optical Engineering, Nanjing University of Science and Technology, where he is also the Leader of the Radar and High-Speed Digital Signal Processing (R&H) Laboratory. He has authored or coauthored four books and more than 100 articles. His current research interests include radar systems, radar signal theory, and digital signal processing. He was a ten-time recipient of the Ministerial and Provincial-Level Science and Technology Award.

XUEHUA LI received the Ph.D. degree in signal and information processing from the University of Electronic Science and Technology of China (UESTC), Chengdu, in 2013. From June 2016 to July 2017, he was a Visiting Scholar with the Department of Electronics Engineering, Colorado State University, Fort Collins, USA. He is currently a Professor with the College of Electronics Engineering, Chengdu University of Information Technology, Chengdu. His current research interests include radar signal processing, weather radar systems, and high-speed digital signal processing.

• • •